AIP Conference Proceedings

RESEARCH ARTICLE | JUNE 21 2016

Hydromagnetic mixed convection flow over an exponentially stretching sheet with fluid-particle suspension FREE

Siti Nur Haseela Izani; Anati Ali

Check for updates

AIP Conf. Proc. 1750, 030043 (2016)
https://doi.org/10.1063/1.4954579

View Online Export Citation

18 June 2024 18:15:48

AIP Advances
Why Publish With Us?
25 DAYS average time to 1st decision
740+ DOWNLOADS average per article
INCLUSIVE scope
Learn More
AIP Publishing

AIP Publishing

Hydromagnetic Mixed Convection Flow over an Exponentially Stretching Sheet with Fluid-Particle Suspension

Siti Nur Haseela Izani[1, a)] and Anati Ali[1, b)]

[1] *Department of Mathematical Sciences,Faculty of Science*
Universiti Teknologi Malaysia, 81310 Johor Bahru, Malaysia

[a)] Corresponding author: snhaseela_izani@yahoo.com
[b)]anati@utm.my

Abstract. The present paper deals with the study of a convective heat transfer characteristics of an incompressible viscous dusty fluid over an exponentially stretching surface with an exponential temperature distribution. The similarity transformation is used to reduce the system of governing partial differential equations into a set of non-linear ordinary differential equations which is then solved numerically using Runge-Kutta-Fehlberg fourth-fifth method (RKF45) with the help of Maple. The influence of physical parameters such as the Prandtl number, mixed convection parameter, the local fluid-particle interaction parameter, Eckert number and the magnetic parameter on the flow and heat transfer characteristics are analyzed and discussed in details through tables and graphs. The behavior of velocity and temperature profile of hydromagnetic mixed convection flow with fluid-particle suspension are assumed to have specific exponential function forms. The present numerical results are compared with the earlier published results.

18 June 2024 18:15:48

INTRODUCTION

The study of flow and heat transfer in the boundary layer of continuous stretching surface has attracted considerable attention because of its large number of applications in engineering and industry processes. Metallurgy for the metal processing like metal spinning, artificial fibers, drawing of plastic films and polymer extrusion etc. are some example of applications related to this study. In view of this, Sakiadis [1] who studied the stretching flow problem encourages many researchers engaged with the problem of boundary layer flow in order to obtain the thermal and kinematic behaviors by considering the different forms of stretching velocity. Magyari and Keller [2] have studied the similarity solutions on heat and mass transfer analysis on boundary layer flow due to an exponentially continuous stretching sheet. Ishak [3] investigated the hydromagnetic boundary layer flow over an exponentially stretching sheet in the presence of radiation. Also, Sajid and Hayat [4] solved analytically on the problem of steady laminar two-dimensional boundary layer flow and heat transfer with the effect of thermal radiation due to an exponentially stretching sheet. Later, the same problem has been solved numerically by Bidin and Nazar [5]. Recently, by considering the effect of buoyancy, Pal [6] studied the effect of magnetic field in the mixed convection flow past an exponentially stretching sheet. Srinivasacharya and Ramreddy [7] analyzed the Soret and Dufour effects on mixed convection of viscous flow due to an exponentially stretching sheet.

In all the studies mentioned above, the authors only considered the fluid flow induced by an exponentially stretching sheet with an absence of fluid-particle suspension. In fact, the problem of the fluid flow embedded with dust particles has gained increased attention due to its various applications in the problem of dispersion and fall-out of pollutants in air and water. Safmann [8] initially formulated governing equations for the flow of dusty fluid in his study on the stability of laminar flow of a dusty gas in which dust particles are uniformly distributed. He encourages some authors to investigate the various aspects of this problem. Siddiqa *et.al* [9] investigated the numerical solution of a dusty fluid boundary layer problem past a vertical plate by considering such three important two-phase mechanisms. Meanwhile, Gireesha *et al.* [10] investigated the steady dusty fluid considering the heat transfer over a

Advances in Industrial and Applied Mathematics
AIP Conf. Proc. 1750, 030043-1–030043-10; doi: 10.1063/1.4954579
Published by AIP Publishing. 978-0-7354-1407-5/$30.00

stretching sheet. Gireesha *et al.* [11] had investigated magnetohydrodynamic boundary layer flow and heat transfer of a dusty fluid over a stretching sheet with viscous dissipation.

Recently, the interest on dusty fluid considering exponentially stretching sheet have been critically analyzed by many authors. Gireesha *et.al* [12] studied the effects of magnetic field on boundary layer flow and heat transfer of a dusty fluid over an exponentially stretching sheet with an exponential temperature distribution. Meanwhile, Pavithra and Gireesha [13] studied the effects of internal heat generation or absorption on dusty fluid flow past an exponentially stretching sheet with viscous dissipation. Some study has been carried out to analyze the problem of convective heat transfer in a dusty fluid over a vertical permeable surface with thermal radiation by Ramesh *et.al* [14]. Also, Gireesha *et.al* [15] studied the effects of variable non-uniform heat source and thermal radiation on mixed convective flow and heat transfer of dusty fluid over a stretching sheet.

To the best of author's knowledge, studies on mixed convection flow and heat transfer on hydromagnetic dusty fluid flow over an exponentially stretching sheet have not been considered so far. The buoyancy effects and the dimensionless distance along the plate are taken into consideration for this mathematical analysis. The governing equations are transformed into set of non-linear ordinary differential equation by using the similarity variables and then solved numerically using RKF45 scheme with the help of Maple software. The influence of physical parameters on the flow and heat transfer characteristics are analyzed and discussed in details through tables and graph. The present numerical results are compared with the earlier published results. It is believed that the results of this study can be used and developed for several multiphase theories which can be obtained from the problem of exhaust nozzle of rockets using solid propellant with added metal powder, coating industry, paint spraying, conveying of powder material in blood vessels and the prediction of particulate deposition from urban atmospheric gas emissions.

MATHEMATICAL FORMULATION

Consider a steady two dimensional laminar boundary layer flow of an incompressible viscous dusty fluid and convective heat transfer near an impermeable exponential sheet stretching with velocity $U_w(x)$ and temperature $T_w(x)$. The flow moving through a quiescent ambient fluid of constant temperature T_∞. The *x*-axis is directed along the continuous stretching sheet and points in the direction of motion and *y*-axis is perpendicular to it. In addition, the convection are considered and also a uniform magnetic field is assumed to be applied in the direction perpendicular to the stretching surface.

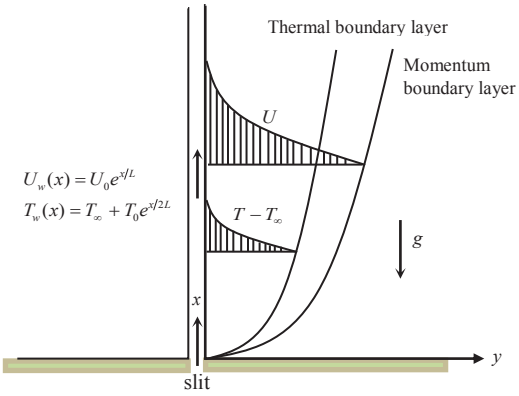

FIGURE 1. Schematic diagram of the flow geometry.

Using the usual Boussinesq's and boundary layer approximations, the governing equations for steady flow dusty fluid consist of two sets of equations for fluid and dust phase as follows

Fluid phase:

$$\frac{\partial u}{\partial x} + \frac{\partial v}{\partial y} = 0 \tag{1}$$

18 June 2024 18:15:48

$$u\frac{\partial u}{\partial x}+v\frac{\partial v}{\partial y}=\upsilon\frac{\partial^2 u}{\partial y^2}+\underbrace{\frac{KN}{\rho}(u_p-u)}_{\text{fluid-particle interaction}}-\underbrace{\frac{\sigma B^2 u}{\rho}}_{\text{magnetic field}}+\underbrace{g\beta^*\left(T-T_\infty\right)}_{\text{mixed convection}} \tag{2}$$

$$u\frac{\partial T}{\partial x}+v\frac{\partial T}{\partial y}=\frac{\kappa}{\rho c_p}\frac{\partial^2 T}{\partial y^2}+\frac{N}{\rho\tau_T}(T_p-T)+\frac{N}{\rho c_p\tau_v}(u_p-u)^2 \tag{3}$$

Dust Phase:

$$\frac{\partial u_p}{\partial x}+\frac{\partial v_p}{\partial y}=0 \tag{4}$$

$$u_p\frac{\partial u_p}{\partial x}+v_p\frac{\partial u_p}{\partial y}=\frac{K}{m}(u-u_p) \tag{5}$$

$$Nc_m\left(u_p\frac{\partial T_p}{\partial x}+v_p\frac{\partial T_p}{\partial y}\right)=-\frac{Nc_p}{\tau_T}(T_p-T) \tag{6}$$

where (u,v) and (u_p,v_p) are the velocity components of the fluid and particle phase along x and y, respectively represents coordinate axes along the continuous surface in the direction of motion and perpendicular to it, υ is the coefficient of viscosity of fluid, N denotes number density of the dust particles, ρ is the density of the fluid phase, K is the Stoke's resistance, g is the acceleration due to the gravity, β^* is the coefficient of thermal expansion, σ is the electrical conductivity, B denotes the strength of the magnetic field, $\tau_v=m/K$ is the relaxation time of dust phase (time required by dust particle to adjust its velocity relative to the fluid), T and T_p are the temperatures of the fluid and dust particle inside the boundary layer, T_∞ is the temperature of the fluid far away from the plate, c_p and c_m are the specific heat of fluid and dust particles, κ is the thermal conductivity and τ_T is the thermal equilibrium time (time required by a particle cloud to adjust its temperature to the fluid).

In order to solve the governing boundary layer equations, we employ the boundary conditions on velocity and temperature fields:

$$\begin{aligned}&u=U_w(x),\quad v=0,\quad T=T_w(x)\qquad \text{at } y=0,\\ &u\to 0,\quad u_p\to 0,\quad v_p\to v,\quad T\to T_\infty,\quad T_p\to T_\infty\ ,\qquad \text{as}\quad y\to\infty.\end{aligned} \tag{7}$$

where $U_w(x)=U_o e^{\frac{x}{L}}$ is the stretching velocity, $T_w(x)=T_\infty+T_o\,e^{\frac{x}{2L}}$ is the exponential temperature distribution and U_0, L, T_o denotes the reference velocity, length and temperature distribution in the stretching surface, respectively. We introduce the following similarity transformation in terms of similarity functions, f and θ, and the similarity variable, η in order to convert the governing equations into set similarity equations as

$$u=U_o e^{\frac{x}{L}} f'(\eta),\qquad v=-\sqrt{\frac{U_o\nu}{2L}}\,e^{\frac{x}{2L}}\left[f(\eta)+\eta f'(\eta)\right],\qquad T=T_\infty+T_0\,e^{\frac{x}{2L}}\,\theta(\eta),$$

$$u_p=U_o e^{\frac{x}{L}} F'(\eta),\qquad v_p=-\sqrt{\frac{U_o\nu}{2L}}\,e^{\frac{x}{2L}}\left[F(\eta)+\eta F'(\eta)\right],\qquad T_p=T_0\,e^{\frac{x}{2L}}\,\theta_p(\eta)+T_\infty,$$

$$\eta=\sqrt{\frac{U_o}{2\nu L}}\,e^{\frac{x}{2L}}\,y,\qquad B=B_0 e^{\frac{x}{2L}},$$

18 June 2024 18:15:48

$$\theta(\eta)=\frac{T-T_\infty}{T_w-T_\infty},\qquad \theta_p(\eta)=\frac{T_p-T_\infty}{T_w-T_\infty}. \tag{8}$$

By employing the similarity equation (8), we identically satisfy equation (1) and (4) and we obtain the following nonlinear ordinary differential equations for (2),(3),(5) and (6):

$$f'''(\eta)+f(\eta)f''(\eta)-2f'(\eta)^2+2\ell\beta\left[F'(\eta)-f'(\eta)\right]-Mf'(\eta)+2Ri\ e^{-3X/2}\,\theta(\eta)=0 \tag{9}$$

$$\theta''(\eta)+\Pr\left[f(\eta)\theta'(\eta)-f'(\eta)\theta(\eta)\right]+2a_1\ \Pr N\left(\theta_p(\eta)-\theta(\eta)\right)+2a_2\ \Pr Ec\,N\left[F'(\eta)-f'(\eta)\right]^2=0 \tag{10}$$

$$F(\eta)F''(\eta)-2F'(\eta)^2+2\beta\left[f'(\eta)-F'(\eta)\right]=0 \tag{11}$$

$$F'(\eta)\theta_p(\eta)-F(\eta)\theta_p'(\eta)+2b_1\left[\theta_p(\eta)-\theta(\eta)\right]=0 \tag{12}$$

where a prime imply differentiation with respect to η, $X=x/L$ is the X-location, $\ell=mN/\rho$ is the mass concentration, $\beta=L\mathrm{e}^{-\frac{x}{L}}/\tau_v U_0$ is the local fluid-particle interaction parameter, $M=2\sigma B_0^{\,2}L/\rho U_0$ is the magnetic parameter, $Ri=Gr/\mathrm{Re}^2$ is the mixed convection parameter, $\mathrm{Re}=u_0L/v$ is the Reynolds number, $Gr=g\beta^*T_0L^3/v^2$ is the thermal Grashof number, $\Pr=\mu C_p/k$ is the Prandtl number, $Ec=U_0^{\,2}/c_pT_0$ is the Eckert number, $a_1=L\mathrm{e}^{-\frac{x}{L}}/\tau_T\rho U_0$ and $b_1=C_pL\mathrm{e}^{-\frac{x}{L}}/\tau_T C_m U_0$ are the local fluid – particle interaction parameter for heat transfer and $a_2=L\mathrm{e}^{\frac{x}{2L}}/\tau_T\rho U_0$ is the local fluid-particle interaction parameter for velocity.

The boundary conditions (7) in terms of f and θ will become

$$\begin{aligned}&f(\eta)=0 \quad f'(\eta)=1 \quad \theta(\eta)=1 \quad \text{at} \quad \eta=0,\\ &f'(\eta)=0, \quad F'(\eta)=0, \quad F(\eta)=f(\eta)+\eta f'(\eta)-\eta F'(\eta), \quad \theta(\eta)\to 0, \quad \theta_p(\eta)\to 0 \quad \text{as} \quad \eta\to\infty.\end{aligned} \tag{13}$$

NUMERICAL SOLUTIONS

Steady, two dimensional, mixed convection flow and heat transfer of a fluid-particle suspension over an exponentially stretching sheet are considered. The system of nonlinear equations (1) to (6) subject to the boundary conditions (7) are converted into a system of non-linear ordinary differential equations using similarity transformation. Then, to seek the numerical solution of this problem, the nonlinear ordinary differential equations (9) to (12) are solved numerically by using RKF45 scheme with the help of Maple [16]. In the present study, the suitable finite values of $\eta\to\infty$ say $\eta\to 5$ were chosen wisely. Numerical solution have been carried out to study the effect of various physical parameter such as fluid-particle interaction parameter β, the magnetic parameter M, mixed convection parameter Ri, X-location parameter, Eckert number Ec and Prandtl number Pr on the flow. We obtained the results for $-\theta'(0)$ in the present works and Table 1 shows the comparative value of $-\theta'(0)$ with Magyari and Keller [2], Elbashbeshy *et.al* [17] and Pal [6] in absence of mixed convection parameter, fluid-particle interaction parameter, effects of various parameters on different profiles at any given X location, number of dust particles, and magnetic field.

TABLE 1. Comparison of results for the dimensionless temperature gradient $-\theta'(0)$ for various values of $\Pr$ in case of $Ri=\beta=X=N=M=0$.

Pr	Magyari and Keller [2]	Elbashbeshy *et. al* [17]	Pal [6]	Present Study
1.0	0.95478	0.95478	0.95478	0.95481
3.0	1.86908	1.86907	1.86907	1.86907
5.0	2.50014	2.50013	2.50013	2.50013
8.0	3.24213		3.24212	3.24212
10.0	3.66038	3.66037	3.66037	3.66037

18 June 2024 18:15:48

In the case of the mixed convection boundary layer flow, Siddiqa and Hosain [18] stated that $Ri = Gr/R\mathrm{e}^2$ (governing parameter for the laminar boundary layer mixed convective flow) represents the ratio of buoyancy forces to the inertial forces inside the boundary layer. To be mentioned here, forced convection exists when the limit of Ri approach to zero and if Ri become large, the limit of free convection can be reached.

RESULTS AND DISCUSSION

The steady mixed convection hydromagnetic boundary layer of a dusty fluid over an exponentially stretching sheet is examined. The velocity $\left(f'(\eta), F'(\eta)\right)$ and the temperature $\left(\theta(\eta), \theta_p(\eta)\right)$ profile for various values of physical parameters are depicted graphically. The present study considers some parameters such as the mixed convection parameter Ri, the local fluid-particle interaction parameter β, magnetic parameter M, X-location parameter X, Prandtl number Pr and Eckert number Ec.

The following default parameter values are used throughout our present study for the numerical computations: $a_1 = 2$, $a_2 = 2$, $b_1 = 1$, $l = 0.1$ and $N = 1$. Figure 2 depicts the variation of velocity profiles with η for different values of the local fluid-particle interaction parameter β for both fluid phase velocity $f'(\eta)$ and dust particle phase $F'(\eta)$. We infer from this figure that the increasing values of β decreases the velocity profile for fluid phase and increases the dust particle phase in the boundary layer. The temperature profile for various values of fluid-particle interaction β is represented in Figure 3. It is noticed from this figure that as the values of β increases, the temperature profiles for both phases decrease.

Figure 4 shows the effects of magnetic field M on velocity profiles for both phases. From this figure, we noticed that the velocity profiles for fluid phase and dust phase decreases as the values of M increases. This is owing to the fact that, the introduction of a transverse magnetic field (normal to the flow direction) has a liability to create the drag known as the Lorentz force which tends to resist the flow [12].

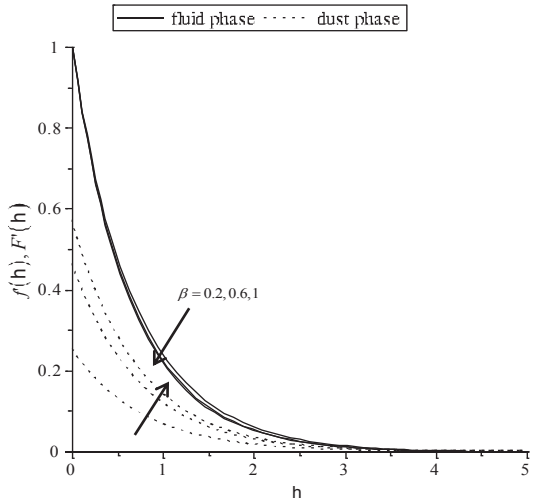

FIGURE 2. Velocity distribution against η for various values of β with $Ec = 2$, $\mathrm{Pr} = 1$, $M = 2$, $Ri = 1$ and $X = 0.5$.

18 June 2024 18:15:48

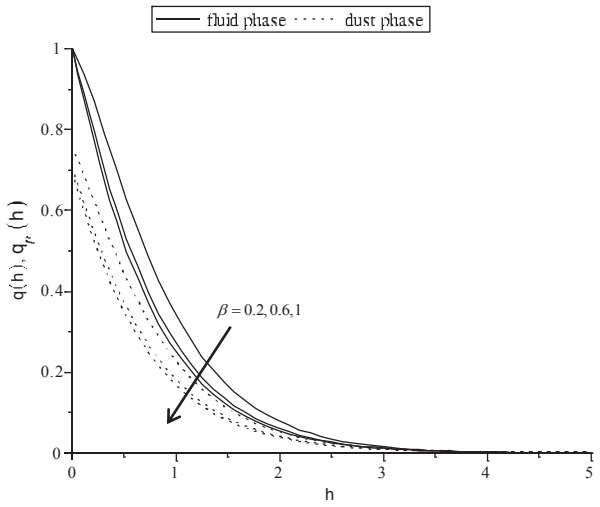

FIGURE 3. Temperature distribution against η for various values of β with $Ec = 2$, $\Pr = 1$, $M = 2$, $Ri = 1$ and $X = 0.5$.

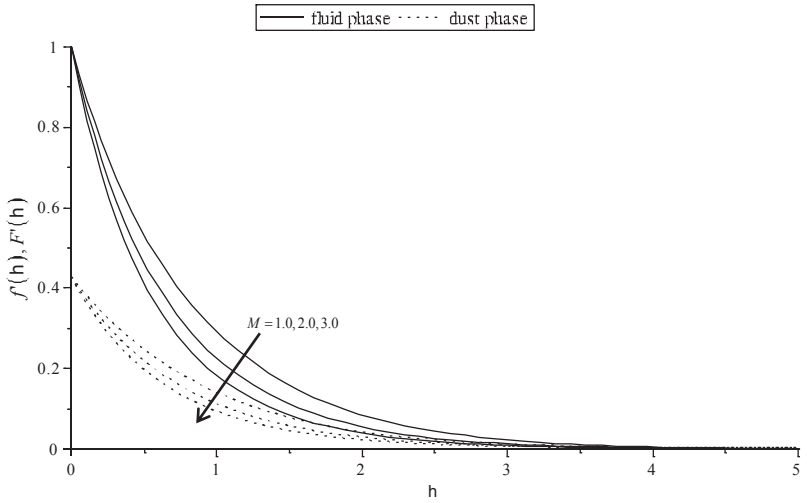

FIGURE 4. Velocity distribution against η for various values of M with $Ec = 2$, $\Pr = 1$, $\beta = 0.5$, $Ri = 1$ and $X = 0.5$.

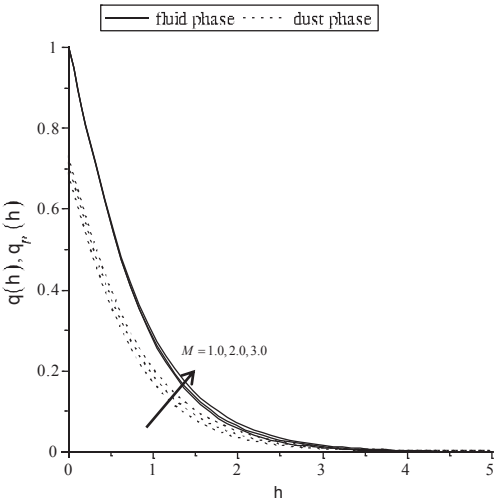

FIGURE 5. Temperature distribution against η for various values of M with $Ec = 2$, $\Pr = 1$, $\beta = 0.5$, $Ri = 1$ and $X = 0.5$.

18 June 2024 18:15:48

The temperature profile for the effects of magnetic field parameter M is represented for both phases in Figure 5. From this figure, it shows that the temperature profile for both fluid phase and dust phase increases with the increase of M. Thus, from this result, it clearly indicates that the transverse magnetic field boost a resistive force (Lorentz Force) of an electrically conducting fluid. The temperature increases as the M increases because the force makes the fluid feels a resistance by increasing the friction between its layers.

Figure 6 explains the temperature profile for different values of Prandtl number Pr. We infer from this figure the increase in the value of Pr decreases the temperature of fluid and dust phase. So that the rate of cooling can be increased by using the Prandtl number. Figure 7 illustrate the effects of Eckert number Ec on temperature profile for both phases. From this figure, it reveals that the temperature increases for both phases with increasing the values of Ec. It is true for this figure due to the fact says the heat energy is stored in the liquid due to frictional heating.

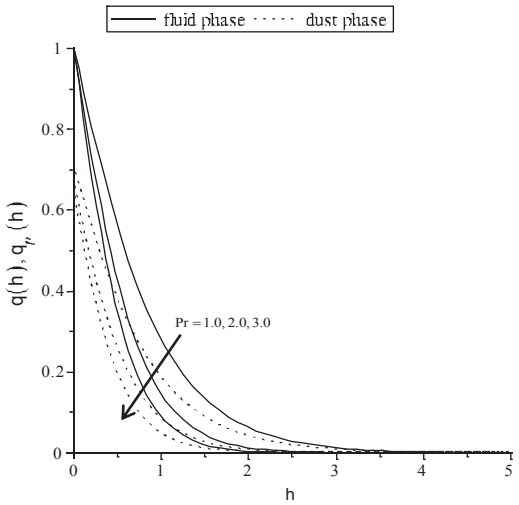

FIGURE 6. Temperature distribution against η for various values of Pr with $Ec = 2$, $\beta = 0.5$, $M = 2$, $Ri = 1$ and $X = 0.5$.

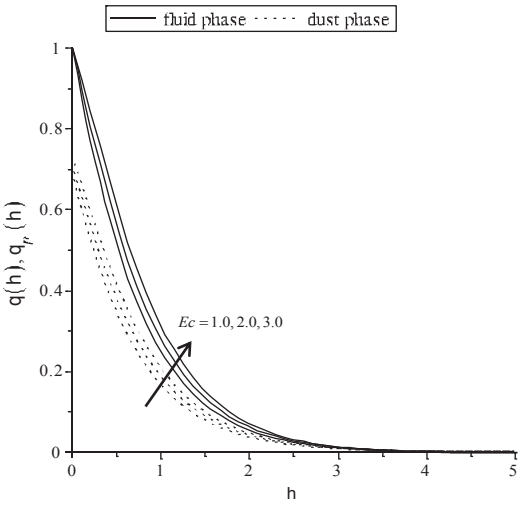

FIGURE 7. Temperature distribution against η for various values of Ec with $\Pr = 1$, $\beta = 0.5$, $M = 2$, $Ri = 1$ and $X = 0.5$.

The observations from Figure 8 shows that as the value of Ri rises, the dimensionless velocity of fluid and dust particles increases. The fluid flow in case of mixed convection increases as the Ri (i.e buoyancy effects) increases. Compared with the pure forced convection case (i.e $Ri = 0.0$), the velocity is more for aiding flow and less for opposing flow.

As Ri enhances, it can be noticed from Figure 9 that the dimensionless temperature of fluid and dust particles decreases. Thus, it is obviously different with Figure 8 as for this case, the temperature is less for aiding flow and is more for opposing flow compared to that of pure forced convection. It should be mention that, the temperature decline and the convection cooling effect increases due to the increment of values Ri (i.e buoyancy effect).

18 June 2024 18:15:48

In Figure 10 and 11, the effect of the X -location on the dimensionless velocity and temperature are delineated for constant values of Pr , M , Ri , Ec and β . Figure 10 shows that a rise in X values in the momentum boundary layer substantially decrease the velocity for both phases. Meanwhile, it is noticed that the temperature increases with an increase in the value of X for both phases.

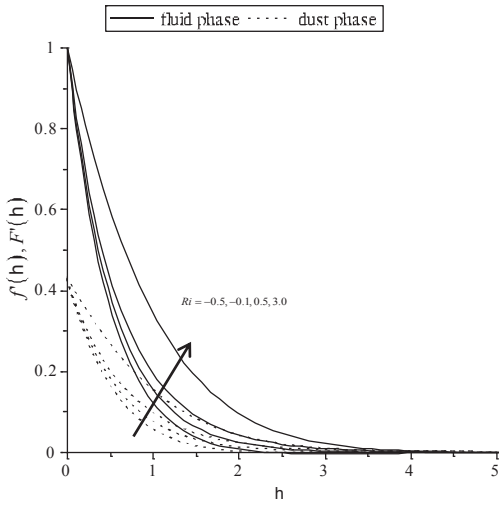

FIGURE 8. Velocity distribution against η for various values of Ri with $Ec = 2$, $\Pr = 1$, $\beta = 0.5$, $M = 2$ and $X = 0.5$.

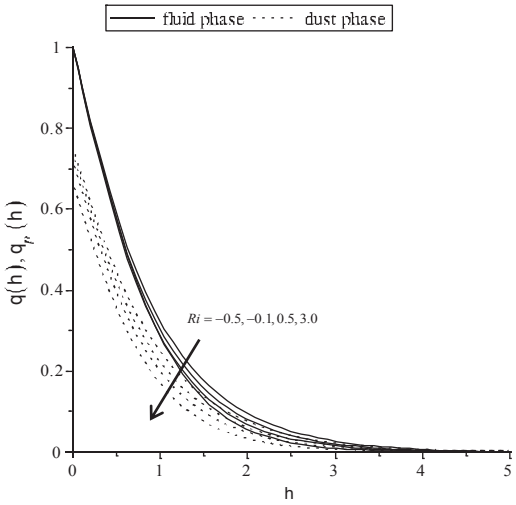

FIGURE 9. Temperature distribution against η for various values of Ri with $Ec = 2$, $\Pr = 1$, $\beta = 0.5$, $M = 2$ and $X = 0.5$.

18 June 2024 18:15:48

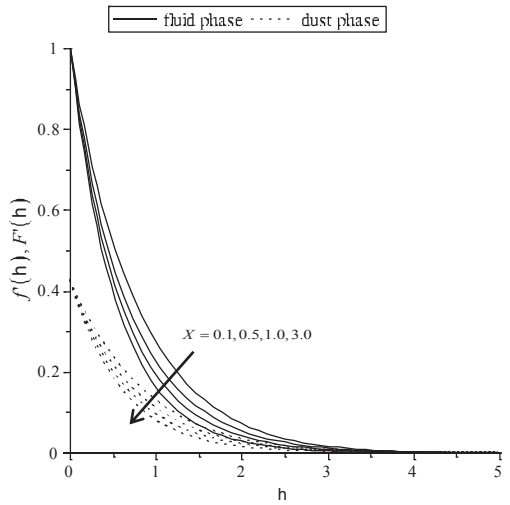

FIGURE 10. Velocity distribution against η for various values of X with $Ec = 2$, $\Pr = 1$, $\beta = 0.5$, $M = 2$ and $Ri = 1$.

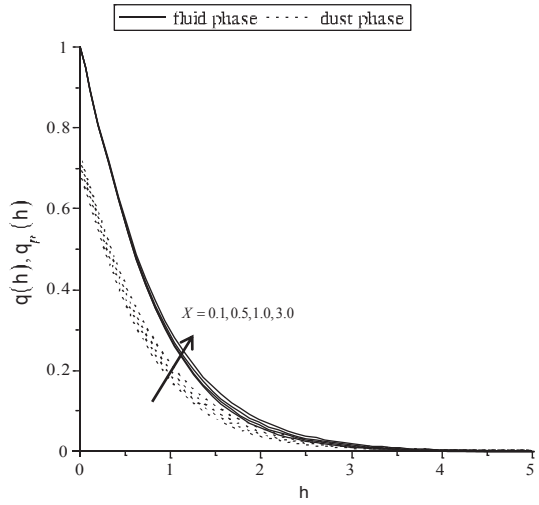

FIGURE 11. Temperature distribution against η for various values of X with $Ec = 2$, $\Pr = 1$, $\beta = 0.5$, $M = 2$ and $Ri = 1$.

CONCLUSION

Convection heat transfer in hydromagnetic flow over an exponentially stretching sheet with fluid particle suspension has been studied. The buoyancy effects and the dimensionless distance along the plate are taking into consideration for this mathematical analysis. Using the similarity variables, the governing equations are transformed into set of non-linear ordinary differential equation and solved numerically using RKF45 scheme with the help of Maple software. Hence, the numerical solutions have been presented graphically and discussed briefly for different values of parameters such as β, M, $\Pr$, Ec, Ri and X. The summary of these obtained results are shown in Table 2 and Table 3 as below.

TABLE 2. The value of parameters β, M, $\Pr$, Ec, Ri and X to be increase as the behavior of velocity and temperature profiles for both phases increases.

		Parameter to be increased
To increase velocity profile	f'	Ri
	F'	β, Ri
To increase temperature profile	θ	M, Ec, X
	θ_p	M, Ec, X

18 June 2024 18:15:48

TABLE 3. The value of parameters β , M , Pr , Ec , Ri and X to be increase as the behavior of velocity and temperature profiles for both phases decreases.

		Parameter to be increased
To decrease velocity profile	f'	β , M , X
	F'	M , X
To decrease temperature profile	θ	β , Pr , Ri
	θ_p	β , Pr , Ri

These results might be useful in controlling the velocity and temperature distributions for problems fluid flow involving fluid-particles suspensions.

ACKNOWLEDGMENTS

The authors are very much thankful to the reviewers for their encouraging comments and suggestions to improve the presentation of this paper.

REFERENCES

1. B. C. Sakiadis, AIChE Journal. **7**(1), 26-28 (1961).
2. E. Magyari and B. Keller, Journal of Physics D: Applied Physics. **32**(5), 577 (1999).
3. A. Ishak, Sains Malaysiana. **40**(4), 391-395 (2011).
4. M. Sajid and T. Hayat, International Communications in Heat and Mass Transfer. **35**(3), 347-356 (2008).
5. B. Biliana and N. Roslinda, European Journal of Scientific Research. **33**(4), 710-717 (2009).
6. D. Pal, Applied Mathematics and Computation. **217**(6), 2356-2369 (2010).
7. D. Srinivasacharya and Ch. RamReddy, International Journal of Nonlinear Science. **12**(1), 60-68 (2011).
8. P.G. Saffman, Journal of Fluid Mechanics. **13**(1), 120-128 (1962).
9. S. Siddiqa, M.A. Hossain and S. C. Saha, International Journal of Numerical Methods for Heat & Fluid Flow. **25**(7), 1542-1556 (2015).
10. B. J. Gireesha, G. K. Ramesh, H. J. Lokesh and C.S. Bagewadi, Applied Mathematics. **2**(4), 475 (2011).
11. B. J. Gireesha, G. K. Ramesh and C. S. Bagewadi, Journal of Applied Sciences Research. **3**(4), 2392-2401 (2012).
12. B. J. Gireesha, G. M. Pavithra and C. S. Bagewadi, British Journal of Mathematics & Computer Science. **2**(4), 187-197 (2012).
13. G. M. Pavithra and B. J. Gireesha, Journal of Mathematics 2013, (2013).
14. G.K. Ramesh, B. J. Gireesha and C. S. Bagawedi, International Journal of Nonlinear Science. **14**(2), 243-250 (2012).
15. B. J. Gireesha, A. J. Chamkha, S. Manjunatha, and C. S. Bagewadi, International Journal of Numerical Methods for Heat & Fluid Flow. **23**(4), 598-612 (2013).
16. A. Aziz, Communications in Nonlinear Science and Numerical Simulation. **14**(4), 1064-1068 (2009).
17. E. M. Elbashbeshy, T. G. Emam and K. M. Abdelgaber, Journal of the Egyptian Mathematical Society. **20**(3) 215-222 (2012).
18. S. Siddiqa and M. A. Hossain, Applied Mathematics. **3**, 705-716 (2012).

18 June 2024 18:15:48